Photoionization cross sections of rovibrational levels of the $B\,^1\Sigma_u^+$ state of H_2

H. Rudolph, D. L. Lynch, S. N. Dixit, and V. McKoy
Arthur Amos Noyes Laboratory of Chemical Physics, [a] *California Institute of Technology, Pasadena, California 91125*

(Received 21 February 1986; accepted 7 March 1986)

We report theoretical cross sections for direct photoionization of specific rovibrational levels of the $B\,^1\Sigma_u^+$ electronic state of H_2. The calculated cross sections differ considerably from values recently determined by resonant enhanced multiphoton ionization (REMPI) studies. In an attempt to understand the disagreement, we analyze in detail the REMPI dynamics and find that the multiphoton ionization probability is extremely sensitive to the spatial and temporal profiles of the laser pulses. Accurate characterization of laser profiles and their jitter is therefore necessary for a comparison between theory and experiment.

INTRODUCTION

In recent years, resonant enhanced multiphoton ionization (REMPI) coupled with photoelectron spectroscopy (PES) has become a highly sensitive technique for spectroscopic as well as dynamical studies. In addition to the observation of hitherto unknown excited states, several studies have illustrated important dynamical features such as the non-Franck–Condon behavior in ionic vibrational branching ratios,[1,2] propensity rules in ionic rotational branching ratios,[3,4] Rydberg-valance mixing and predissociation,[5] and strong final state selectivity.[6] REMPI processes are also being used for detection and characterization of species in unimolecular reactions[7] and desorption from surfaces.[8] In addition to the detection of new states, REMPI processes also offer the possibility of measuring photoionization cross sections for excited states. Often such studies probe the part of the photoelectron continuum inaccessible by single photon ionization out of the ground state. Moreover, extraction of absolute REMPI cross sections from measured ion/electron signals requires the knowledge of the atomic/molecular densities in the interaction volume and the characteristics of the laser pulses used. Recent experiments in atomic[9] and molecular[10–12] systems have circumvented these difficulties in measuring absolute particle densities by studying the saturation behavior of the REMPI signal as a function of the laser intensity. Furthermore, measured values of the cross sections for ionization out of the $A\,^2\Sigma^+$ state of NO derived by this technique[10] were seen to be within a factor of 2 of subsequent theoretical studies.[13]

In another, more recent, experiment Meier *et al.*[11] reported cross sections for photoionization out of specific rovibrational levels of the $B\,^1\Sigma_u^+$ state of H_2. These cross sections were extracted by observing the saturation behavior of the ion signal as the intensity of the ionizing laser is varied in their two color (1 + 1) REMPI experiment. We have calculated the relevant cross sections using *ab initio* electronic wave functions and our calculated values are compared with the measured ones[11] in Table I. The experimental values seem to be consistently lower than the theoretical numbers by about an order of magnitude.

In an attempt to understand such a large discrepancy, we analyze the REMPI dynamics in detail using density matrix equations. Some limitations to the use of the rate equations in the analysis of Ref. 11 are discussed. In addition, we show that the REMPI signal is very sensitive to the spatial and temporal profiles of the laser. Proper analysis of the experimental data, therefore, requires a characterization of laser profiles and a subsequent incorporation of these into the dynamics. Laser characteristics for the experiment of Meier *et al.*[11] are needed for further comparison between theory and experiment.

THEORETICAL CALCULATIONS

In this section we discuss the results of our calculations of the ionization probability for the two color (1 + 1)

TABLE I. $B\,^1\Sigma_u^+(v_i, J_i, M_i) \xrightarrow{\hbar\omega} X\,^2\Sigma_g^+ + e^-$ photoionization cross sections (in 10^{-18} cm^2) of H_2 at $\lambda = 266.05$ nm.

			Calculated		Measured[a]
v_i	J_i	M_i	σ_v	σ_L	σ
0	0	0	11.99	12.19	0.83 ± 0.17
0	1	0	13.10	13.65	0.52 ± 0.10
0	1	± 1	11.43	11.46	
0	2	0	12.79	13.23	
0	2	± 1	12.39	12.71	1.19 ± 0.24
0	2	± 2	11.19	11.15	
0	3	0	12.73	13.16	
0	3	± 1	12.55	12.92	0.84 ± 0.17
0	3	± 2	11.99	12.19	
0	3	± 3	11.06	10.98	
3	0	0	5.07	5.03	0.65 ± 0.13
3	1	0	5.55	5.60	0.23 ± 0.05
3	1	± 1	4.84	4.74	
3	2	0	5.41	5.43	
3	2	± 1	5.24	5.23	1.03 ± 0.20
3	2	± 2	4.73	4.62	
3	3	0	5.39	5.41	
3	3	± 1	5.31	5.31	
3	3	± 2	5.07	5.03	0.25 ± 0.05
3	3	± 3	4.68	4.55	

[a] Reference 11.

[a] Contribution No. 7368.

 0021-9606/86/126657-05$02.10

REMPI process in H_2 via the $B\,^1\Sigma_u^+$ state

$$H_2(X\,^1\Sigma_g^+,\ v_0=0,\ J_0)\xrightarrow{\hbar\omega_1} H_2^*(B\,^1\Sigma_u^+,\ v_i=0,3,\ J_i)$$

$$\xrightarrow{\hbar\omega_2} H_2^+(X\,^2\Sigma_g^+)+e^-. \qquad (1)$$

The parameters required for the analysis of the dynamics of this REMPI process are, the X–B transition moment, the decay rates out of the B state, and photoionization cross sections out of specific rotational–vibrational levels of the B state. We have used the X–B transition moments given by Wolniewicz[14] and vibrational wave functions obtained by the finite element method[15] using the potential curves of Sharp.[16] The spontaneous decay rate of the B state is taken to be $1.85\times10^9\ s^{-1}$.[11,17] The electronic wave functions of the B state at various internuclear separations (R) were calculated using the improved virtual orbital (IVO) technique[18] with sufficient number of diffuse functions included in the basis set. The resulting energies of the $B\,^1\Sigma_u^+$ state are within 5%–10% of the accurate values.[16] As an additional check on the quality of the wave functions, the X–B transition moments were calculated and agree with those of Wolniewicz[14] to within 7% up to $R=2.0$ a.u. For larger R, the deviation between our values and the accurate ones increases because of the single configuration wave functions used by us. We believe, however, that for the vibrational states under consideration in the photoionization step, these large R errors will play a less significant role in the averaged bound–free transition moments. For the bound–bound moments necessary for the REMPI dynamics, we have used the accurate values of Wolniewicz.[14]

The photoelectron continuum wave functions were calculated within the frozen core Hartree–Fock approximation using the iterative Schwinger variational method.[19] Combining these with the B state wave functions, the photoionization dynamical coefficients were calculated. We explicitly included both the energy and R dependence of these dynamical coefficients in averaging over the vibrational wave functions.[20] Finally, the photoionization cross sections for ionization out of specific $|v_i,\ J_iM_i\rangle$ levels of the B state are calculated using the detailed expression given in an earlier paper.[21] Since Meier *et al.*[11] collected total ion signals, we have summed the cross sections over the symmetry allowed ionic rotational states and energetically allowed ionic vibrational states. The results are presented in Table I together with the experimentally deduced cross sections of Ref. 11. The agreement between the length and the velocity forms of cross sections indicates that the single determinant description of the B state as well as of the photoelectron continuum is sufficiently accurate. Moreover, calculations similar to those outlined here (different rovibrational states and kinetic energies but same basis set) have yielded good agreement with measured ionic vibrational–rotational branching ratios.[22] This leads us to believe that, within our model, the theoretical cross sections quoted in Table I are fairly accurate.

As seen from Table I, there is clearly a disagreement between our calculated cross sections and the experimentally deduced values of Meier *et al.*[11] The theoretical values are consistently higher than the experimental ones. Our calculations have not included autoionization. Although the influence of interference with competing autoionizing channels may account for the discrepancy for single rotational/vibrational levels, we feel that it is unlikely to explain the systematic differences observed. Several recent studies[23–25] have demonstrated the sensitivity of REMPI signals to the dynamics and to the spatial-temporal characteristics of the laser employed. We believe that such effects could have influenced the results of Meier *et al.*[11] In the following section we address these questions.

REMPI DYNAMICS

In the experiment of Meier *et al.*[11] a low intensity laser was used for the X–B excitation while a (variable) high intensity laser was used to ionize the B state. The choice of frequencies and intensities eliminates the possibility of excitation by the high intensity laser and ionization by the low intensity one. Focusing on the case where both lasers were linearly polarized along the same direction, collision free conditions imply that the REMPI process originating from each $|J_0M_0\rangle$ state forms an independent channel. The dynamics in each channel can be accurately described by the appropriate density matrix equations. These have been discussed by several authors[12,21] and we will simply reproduce them here in the rotating wave approximation (RWA) for on-resonance excitation:

$$\dot\rho_{00}=-i\tfrac{1}{2}\Omega_{0i}(\rho_{0i}-\rho_{i0})+\alpha\rho_{ii}, \qquad (2a)$$

$$\dot\rho_{ii}=i\tfrac{1}{2}\Omega_{0i}(\rho_{0i}-\rho_{i0})-(\Gamma_i+\alpha)\rho_{ii}, \qquad (2b)$$

$$\dot\rho_{0i}=i\tfrac{1}{2}\Omega_{0i}(\rho_{ii}-\rho_{00})-\tfrac{1}{2}(\Gamma_i+\alpha)\rho_{0i}, \qquad (2c)$$

$$\dot\rho_{i0}=-i\tfrac{1}{2}\Omega_{0i}(\rho_{ii}-\rho_{00})-\tfrac{1}{2}(\Gamma_i+\alpha)\rho_{i0}. \qquad (2d)$$

In the above equations, $\alpha(=1.85\times10^9\ s^{-1})$ denotes the spontaneous decay rate from the B state ($|J_iM_i\rangle\equiv|i\rangle$) to the X state ($|J_0M_0\rangle\equiv|0\rangle$), Ω_{0i} the Rabi frequency for the $|0\rangle-|i\rangle$ transition and Γ_i the ionization rate out of $|i\rangle$. The latter two parameters are laser intensity dependent and can be written as

$$\tfrac{1}{2}\Omega_{0i}=\frac{E_1(t)}{\hbar}\langle 0|\,\boldsymbol{\mu}\cdot\boldsymbol{\epsilon}_1|i\rangle \qquad (3a)$$

and

$$\Gamma_i=\sigma_i\frac{I_2(t)}{\hbar\omega_2}, \qquad (3b)$$

where $\boldsymbol{\mu}$ is the electronic dipole moment operator, $E_1(t)$ is the field envelope of the exciting laser, and $I_2(t)$ is the intensity of the ionizing laser. Detailed expressions for σ_i, the photoionization cross section, and the bound–bound dipole matrix element $\langle 0|\boldsymbol{\mu}\cdot\boldsymbol{\epsilon}_1|i\rangle$ have been given in Ref. 21. Both Ω_{0i} and Γ_i are M dependent quantities and, as such, the saturation behavior of each M_0 channel will be different. The total ionization probability is given by

$$P=1-\sum_{M_0}[\rho_{00}^{M_0}(t)+\rho_{ii}^{M_0}(t)]. \qquad (4)$$

We will discuss the effect of different saturation behavior of M channels in a later publication. For simplicity, here we will treat the $P(1)$ $v_0=0-v_i=3$ excitation case where only one M channel ($M_0=0$) exists.

Under conditions when the time rate of change of ρ_{0i} and ρ_{i0} is small, ρ_{i0} and ρ_{0i} can be adiabatically eliminated from Eq. (2) and one can obtain two rate equations for ρ_{00} and ρ_{ii}. As has been derived by Meier *et al.*[11] and by Rotke *et al.*,[12] these can be written as

$$\dot{\rho}_{00} = W_1(\rho_{ii} - \rho_{00}) + \alpha\rho_{ii}\,, \tag{5a}$$

$$\dot{\rho}_{ii} = -W_1(\rho_{ii} - \rho_{00}) - (W_2 + \alpha)\rho_{ii}\,, \tag{5b}$$

where

$$W_1 = \frac{\Omega_{0i}^2}{\Gamma_i + \alpha} \tag{6}$$

and $W_2 = \Gamma_i$. It is important to note that W_1 depends on W_2. Equation (5) can be solved analytically for a uniform intensity pulse turned on at $t = 0$ and off at τ_p and the ionization probability $P = 1 - \rho_{ii} - \rho_{00}$ can be written as

$$P(\tau_p) = \left[1 - \frac{a+b}{2b}\, e^{-(a-b)\tau_p} + \frac{a-b}{2b}\, e^{-(a+b)\tau_p}\right], \tag{7}$$

where

$$a = W_1 + \frac{W_2 + \alpha}{2} \tag{8a}$$

and

$$b = [a^2 - W_1 W_2]^{1/2}. \tag{8b}$$

A Taylor expansion of $P(\tau_p)$ to first order in W_1 yields Eq. (1) of Meier *et al.*,[11] viz.

$$P(\tau_p) = \frac{W_1}{W_2 + \alpha}\,\tau_p W_2 \left[1 + \frac{e^{-(W_2+\alpha)\tau_p} - 1}{(W_2 + \alpha)\tau_p}\right] \tag{9}$$

which, because of $\alpha\tau_p \approx 9.25 \gg 1$ ($\tau_p = 5$ ns), reduces to

$$P(\tau_p) = \frac{W_1}{W_2 + \alpha}\,\tau_p W_2. \tag{10}$$

While this is identical to Eq. (2) of Ref. 11, an important difference in the analysis arises by realizing that W_1 is a function of W_2 as shown in Eq. (6). The dependence of P on W_2 is then

$$P(\tau_p) = \frac{\Omega_{0i}^2}{(W_2 + \alpha)^2}\,\tau_p W_2 \tag{11}$$

or

$$P^{-1} = \frac{W_2^2 + 2W_2\alpha + \alpha^2}{\Omega_{0i}^2\tau_p \cdot W_2} = \frac{W_2}{\Omega_{0i}^2\tau_p} + \frac{2\alpha}{\Omega_{0i}^2\tau_p} + \frac{\alpha^2}{\Omega_{0i}^2\tau_p \cdot W_2}. \tag{12}$$

Clearly this is in disagreement with Eq. (3) of Ref. 11 used in their analysis which is a result of ignoring the W_2 dependence in W_1. Equation (12) predicts a linear dependence of P^{-1} on W_2^{-1} only for W_2 small compared to α while P^{-1} increases with W_2 for large W_2. Such a decrease of P with increasing W_2 is a consequence of the dynamics and has actually been observed in a two color (2 + 1) REMPI experiment in sodium.[25] It should be noted that such a decrease in the ion signal with increasing intensity will not arise in single color REMPI or when the two pulses do not overlap in time. The observation of a linear dependence of the inverse ion signal on the inverse of the ionizing pulse energy by Meier *et al.*[11] then implies that the intensities used must correspond to $\Gamma_i \ll \alpha$. In the linear regime,

$$P^{-1} = \frac{2\alpha}{\Omega_{0i}^2\tau_p} + \frac{\alpha^2}{\Omega_{0i}^2\tau_p}\,\frac{\hbar\omega_2\tau_p A}{\sigma_i E_2}, \tag{13}$$

where we have used the relation

$$E_2 = I_2 \cdot \tau_p \cdot A \tag{14}$$

between the ionizing laser pulse energy E_2, its intensity I_2, the (rectangular) pulse duration τ_p, and the (uniform intensity) beam cross section area A. A more careful analysis of the Taylor expansion of Eq. (7) will add a correction term $2\Omega_{0i}^2$ to α^2 in the second term in Eq. (13). The cross section can be calculated from the intercept and the slope of the linear part of P^{-1} vs E_2^{-1} graph using

$$\sigma_i = \frac{\text{intercept}}{\text{slope}} \cdot \hbar\omega_2 \alpha A \tau_p \cdot \frac{\alpha^2 + 2\Omega_{0i}^2}{2\alpha^2}. \tag{15}$$

Note that the third factor, absent in the analysis of Ref. 11, reduces the apparent cross section by about a factor of 2.

In Fig. 1, we compare the solution of the density matrix equations (2) with the solution of rate equations (5) for the $v_i = 3$ $P(1)$ excitation. The molecular parameters were calculated as mentioned in the previous section. In relating E_2 to I_2 in Eq. (14) we have used $\tau_p = 5$ ns and $A = 0.01\pi$ mm^2 quoted in Ref. 11. Both methods predict a linear regime for low E_2 and a diverging P^{-1} for high E_2. However, the slopes of the two linear parts are different. This is a result of Ω_{0i} not being much smaller than α ($\Omega_{0i} = 2.5\times10^8$ rad/s, $\alpha = 1.85\times10^9$ s^{-1}). More interestingly, we see that the linear regime exists for pulse energies less than 0.25 mJ or so, whereas Meier *et al.*[11] have observed linear behavior for E_2 up to 2 mJ. This could be a result of using inaccurate values of A and τ_p and not incorporating the spatial and temporal

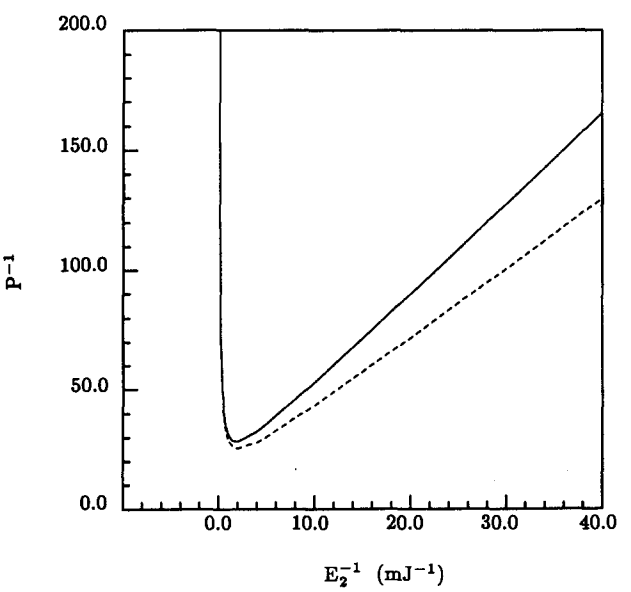

FIG. 1. Inverse of the ionization probability (P^{-1}) a function of the inverse of the ionizing pulse energy. The X–B excitation is through the $v_0 = 0 \rightarrow v_1 = 3$ $J_0 = 1 \rightarrow J_i = 0$ line. (—) density matrix solution, (- - -) rate equation solution. Uniform spatial and temporal profiles are assumed.

profiles of the laser. For uniform pulses, Eq. (15) implies that for a given value of (intercept/slope), the smaller the value of $A\tau_p$, the smaller the calculated cross section.

Since the actual temporal and spatial profiles of the lasers used have not been presented in Ref. 11, we shall assess the influence of these on the dependence of the ionization probability on the ionizing laser pulse energy. For nonuniform pulses, analytical solutions are not possible and therefore we have numerically integrated Eq. (2).

To discuss the effects of temporal pulse shape, we have integrated the density matrix equations (2) assuming Gaussian shaped exciting and ionizing pulses with FWHM $= \tau_p$. The results are displayed in Fig. 2 where we have also illustrated situations where the exciting laser pulse peaks before the ionizing laser peaks (+ jitter) and where the ionizing pulse peaks before the exciting pulse (− jitter). The jitter is fixed at $\pm$ 1 ns.[11] In reality, the jitter is probably a random variable changing from pulse to pulse in which case an averaging of P over the distribution of jitter has to be carried out. The ionization probability in the linear regime is seen to be more sensitive to the jitter than to the Gaussian nature of the pulse shape. Pulse shapes other than Gaussian would be expected to have a profound effect on the resulting ion signal. The spread between + and − jitters gives a measure of the uncertainty in the experimental measurements.

As for the effects of the spatial profile of the laser pulses, we find that a Gaussian spatial profile, as would be for a laser operating in a TEM_{00} mode, has a minor effect on the ion signal. However, as discussed in a later publication,[12] the ionizing laser seems to have an Airy function dependence on the transverse radius in the far-field region, i.e.,

$$I_2(x) = I_0\left(\frac{2J_1(x)}{x}\right)^2, \tag{16}$$

where $J_1(x)$ is the Bessel function of first kind of order one and x is a normalized transverse coordinate.[26] If we equate the energy contained in the central maximum of Eq. (16) to that contained in a uniform distribution of the same radius, we find that the peak intensity (at $x = 0$) in Eq. (16) is about 4.38 times higher than the peak intensity for a uniform intensity pulse. The influence of spatial variation is included by averaging $P[I_2(r)]$ over the distribution

$$\overline{P} = 2\pi \int_0^{\omega_0} P[I_2(r)]\, r\, dr/\pi\omega_0^2, \tag{17}$$

where ω_0 denotes the beam radius [taken to be the first zero of Eq. (16)]. The results are presented in Fig. 3. We see that an Airy function pulse is less efficient in ionization than a uniform pulse. This is because, although the intensity is much higher at the center, it is smaller than the uniform value over a larger area. The averaging is seen to reduce the slope and raise the intercept of the linear part. As in the case relating to the temporal profile, different spatial profiles will also have different effects on the averaged ion signal.

Finally, we should mention that a uniform spatial profile has been assumed for the exciting laser in the above calculations. Inclusion of the actual profile of this laser will undoubtedly give rise to additional changes. Although the exciting laser in Ref. 11 was ten times wider than the ionizing laser, the perpendicular propagation configuration used in that experiment actually probes the complete profiles of both lasers. A co/counter propagating geometry would make the broad exciting laser to appear to have a uniform profile.

CONCLUSIONS

We have presented photoionization cross sections for single-photon ionization of specific rovibrational levels of the $B\,^1\Sigma_u^+$ state of H_2 at $\lambda = 266.05$ nm. Good agreement between the length and velocity forms leads us to believe that these values are fairly accurate. However, recent measured

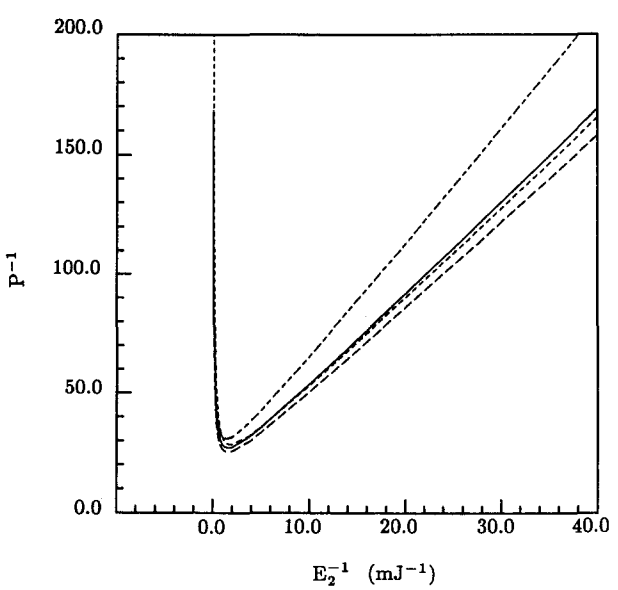

FIG. 2. Same as Fig. 1. (—) Gaussian temporal profile, no jitter; (- - -) uniform temporal profile, no jitter; (– – –) Gaussian temporal profile, + 1.0 ns jitter; (– - – -) Gaussian temporal profile, − 1.0 ns jitter. Uniform spatial profiles are assumed.

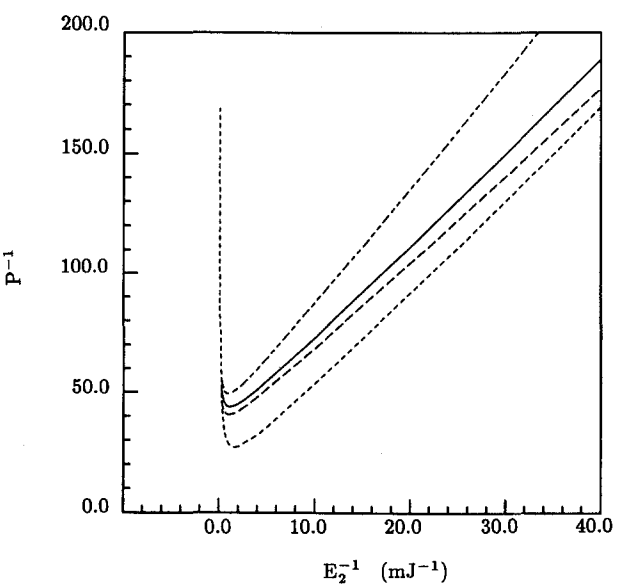

FIG. 3. Same as Fig. 1. (—) Airy function spatial profile no jitter, (- - -) uniform spatial profile no jitter, (– – –) Airy function spatial profile + 1.0 ns jitter, (– - – -) Airy function spatial profile, − 1.0 ns jitter. Gaussian temporal profiles are assumed.

values seem to be consistently lower than our calculated ones for all the levels considered. Although we have not included effects of autoionization, it is unlikely that their incorporation will lower all the calculated cross sections of Table I. On the other hand, we have shown through detailed dynamical calculations that the ion signal is very sensitive to the spatial and temporal profiles of the laser pulses and also to the jitter between the exciting and ionizing pulses. Lacking detailed information on these characteristics in the experiment by Meier *et al.*,[11] we have chosen examples to illustrate the sensitivity of the ion signal to these effects. Such information is essential for further comparison between theory and experiment.

ACKNOWLEDGMENTS

This research was supported by the National Science Foundation under Grant No. CHE8218166. One of us (H.R.) gratefully acknowledges support from the Danish Natural Science Research Council and the Carlsberg Foundation.

[1]S. T. Pratt, E. D. Poliakoff, P. M. Dehmer, and J. L. Dehmer, J. Chem. Phys. **78**, 65 (1983).
[2]S. T. Pratt, P. M. Dehmer, and J. L. Dehmer, Chem. Phys. Lett. **105**, 28 (1984).
[3]W. G. Wilson, K. S. Viswanathan, E. Sekreta, and J. P. Reilly, J. Phys. Chem. **88**, 672 (1984).
[4]K. S. Viswanathan, E. Sekreta, E. R. Davidson, and J. P. Reilly (preprint).
[5]A. Sur, C. V. Ramana, W. A. Chupka, and S. D. Colson, J. Chem. Phys. **84**, 69 (1985).
[6]S. T. Pratt, P. M. Dehmer, and J. L. Dehmer, J. Chem. Phys. **80**, 1706 (1984); **81**, 3444 (1984).
[7]See, for example, O. Benoist Dazy, F. Lahmani, C. Lardeux, and D. Solgadi, Chem. Phys. **94**, 247 (1985).
[8]A. H. Burns, Phys. Rev. Lett. **55**, 525 (1985).
[9]U. Heinzman, D. Schinkowski, and H. D. Zeman, Appl. Phys. **12**, 113 (1977); R. V. Ambartzumian, N. P. Furzikov, V. S. Letokhov, and A. A. Puretzky, *ibid.* **9**, 335 (1976); A. V. Smith, J. E. M. Goldsmith, D. E. Nitz, and S. J. Smith, Phys. Rev. A **22**, 577 (1980).
[10]H. Zacharias, R. Schmiedl, and K. H. Welge, Appl. Phys. **21**, 127 (1980).
[11]W. Meier, H. Rotke, H. Zacharias, and K. H. Welge, J. Chem. Phys. **83**, 4360 (1985).
[12]H. Rotke and H. Zacharias, J. Chem. Phys. **83**, 4831 (1985).
[13]S. N. Dixit, D. L. Lynch, V. McKoy, and W. Huo, Phys. Rev. A **32**, 1267 (1985).
[14]L. Wolniewicz, J. Chem. Phys. **51**, 5002 (1969).
[15]D. J. Malik, J. Eccles, and D. Secrest, J. Comput. Phys. **38**, 157 (1980).
[16]T. E. Sharp, At. Data **2**, 119 (1971).
[17]H. Schmoranzer and J. Imschwiler, Phys. Lett. A **100**, 85 (1984).
[18]W. J. Hunt and W. A. Goddard III, Chem. Phys. Lett. **24**, 464 (1974).
[19]R. R. Lucchese, G. Raseev, and V. McKoy, Phys. Rev. A **25**, 2572 (1982).
[20]S. N. Dixit, D. L. Lynch, and V. McKoy, Phys. Rev. A **30**, 3332 (1984).
[21]S. N. Dixit and V. McKoy, J. Chem. Phys. **82**, 3546 (1985).
[22]D. L. Lynch, S. N. Dixit, and V. McKoy, Chem. Phys. Lett. **123**, 315 (1986).
[23]See, for example, M. Crance, J. Phys. B **13**, 101 (1980).
[24]M. Crance and S. Feneuille, Phys. Rev. A **16**, 1587 (1977).
[25]L. Allen, R. W. Boyd, J. Krasinski, M. S. Malcuit, and C. R. Stroud, Jr., Phys. Rev. Lett. **54**, 309 (1985).
[26]M. Born and E. Wolf, *Principles of Optics*, 6th ed. (Pergamon, New York, 1980), p. 395.